Inorg. Chem. **2006**, *45*, 814–820

Aqueous Ferryl(IV) Ion: Kinetics of Oxygen Atom Transfer To Substrates and Oxo Exchange with Solvent Water

Oleg Pestovsky* and Andreja Bakac*

Ames Laboratory, Iowa State University, Ames, Iowa 50011

Received October 27, 2005

The aqueous iron(IV) ion, $Fe^{IV}_{aq}O^{2+}$, generated from O_3 and Fe_{aq}^{2+}, reacts rapidly with various oxygen atom acceptors (sulfoxides, a water-soluble triarylphosphine, and a thiolatocobalt complex). In each case, $Fe^{IV}_{aq}O^{2+}$ is reduced to Fe_{aq}^{2+}, and the substrate is oxidized to a product expected for oxygen atom transfer. Competition methods were used to determine the kinetics of these reactions, some of which have rate constants in excess of 10^7 M^{-1} s^{-1}. Oxidation of dimethyl sulfoxide (DMSO) has $k = 1.26 \times 10^5$ M^{-1} s^{-1} and shows no deuterium kinetic isotope effect, k(DMSO-d_6) $= 1.23 \times 10^5$ M^{-1} s^{-1}. The $Fe^{IV}_{aq}O^{2+}$/sulfoxide reaction is the product-forming step in a very efficient Fe_{aq}^{2+}-catalyzed oxidation of sulfoxides by ozone. This catalytic cycle, combined with labeling experiments in $H_2{}^{18}O$, was used to determine the rate constant for the oxo-group exchange between $Fe^{IV}_{aq}O^{2+}$ and solvent water under acidic conditions, $k_{exch} = 1.4 \times 10^3$ s^{-1}.

Introduction

Aqueous and coordination chemistry of iron in the oxidation state 4+ has attracted considerable attention in recent years.[1,2] In view of recent discoveries of nonheme iron(IV) participating in several enzymatic systems, i.e., α-ketoglutarate-dependent taurine dioxygenase,[3] methane monooxygenase,[4] and ribonucleotide reductase,[5] considerable synthetic and mechanistic effort has been made toward the isolation and characterization of such species. Several complexes of iron(IV) with amino[6] and amido[7] ligands are sufficiently stable to be characterized by X-ray crystallography. At the same time, such complexes were shown to be strong oxidants, capable even of hydroxylating C−H bonds.[8] In contrast, the chemistry of iron(IV) complexes in the absence of stabilizing ligands remains largely unexplored, despite the role that such complexes may play in Fenton chemistry[9,10] or in some key reactions in the atmosphere and environment.[11,12]

Several decades ago, the reaction between aqueous Fe(II) and oxygen-atom donors, such as HOCl and O_3, was proposed to generate aqueous Fe(IV), eq 1.[13] This species was believed to be extremely short-lived, and the only evidence for its formation in reaction 1 was the observation of dimeric Fe(III), the product of the rapid follow-up step in eq 2.

$$Fe_{aq}^{2+} + SO \rightarrow Fe^{IV}_{aq}O^{2+} + S \qquad SO = O_3, HOCl \quad (1)$$

$$Fe^{IV}_{aq}O^{2+} + Fe_{aq}^{2+} \rightarrow Fe^{III}_{aq}(OH)_2Fe^{III}_{aq}{}^{4+}/2Fe_{aq}^{3+} \quad (2)$$

More recent work focused on spectral and kinetic characterization of $Fe^{IV}_{aq}O^{2+}$ produced in the Fe_{aq}^{2+}/ozone reaction in strongly acidic aqueous solutions, where the

* To whom correspondence should be addressed. E-mail: pvp@iastate.edu. Phone: 515-294-5826 (O.P.) or E-mail: bakac@ameslab.gov. Phone: 515-294-5233 (A.B.).

(1) Costas, M.; Mehn, M. P.; Jensen, M. P.; Que, L., Jr. *Chem. Rev.* **2004**, *104*, 939−986.
(2) Tshuva, E. Y.; Lippard, S. J. *Chem. Rev.* **2004**, *104*, 987−1011.
(3) Price, J. C.; Barr, E. W.; Tirupati, B.; Bollinger, J. M., Jr.; Krebs, C. *Biochemistry* **2003**, *42*, 7497−7508.
(4) Liu, K. E.; Valentine, A. M.; Wang, D.; Huynh, B. H.; Edmondson, D. E.; Salifoglou, A.; Lippard, S. J. *J. Am. Chem. Soc.* **1995**, *117*, 10174−10185.
(5) Sturgeon, B. E.; Burdi, D.; Chen, S.; Huynh, B.-H.; Edmondson, D. E.; Stubbe, J.; Hoffman, B. M. *J. Am. Chem. Soc.* **1996**, *118*, 7551−7557.
(6) Rohde, J.-U.; In, J.-H.; Lim, M. H.; Brennessel, W. W.; Bukowski, M. R.; Stubna, A.; Muenck, E.; Nam, W.; Que, L., Jr. *Science* **2003**, *299*, 1037−1039.
(7) Kostka, K. L.; Fox, B. G.; Hendrich, M. P.; Collins, T. J.; Rickard, C. E. F.; Wright, L. J.; Munck, E. *J. Am. Chem. Soc.* **1993**, *115*, 6746−6757.
(8) Kaizer, J.; Klinker, E. J.; Oh, N. Y.; Rohde, J.-U.; Song, W. J.; Stubna, A.; Kim, J.; Muenck, E.; Nam, W.; Que, L., Jr. *J. Am. Chem. Soc.* **2004**, *126*, 472−473.
(9) Bray, W. C.; Gorin, M. H. *J. Am. Chem. Soc.* **1932**, *54*, 2124−2125.
(10) Kremer, M. L. *J. Phys. Chem. A* **2003**, *107*, 1734−1741.
(11) Hahn, J.; Pienaar, J. J.; Van Eldik, R. *Proc. EUROTRAC Symp. '96: Transp. Transform. Pollut. Troposphere, 4th* **1997**, *1*, 427−431.
(12) Jacobsen, F.; Holcman, J.; Sehested, K. *Int. J. Chem. Kinet.* **1998**, *30*, 215−221.
(13) Conocchioli, T. J.; Hamilton, E. J., Jr.; Sutin, N. *J. Am. Chem. Soc.* **1965**, *87*, 926−927.

10.1021/ic051868z CCC: $33.50
Published on Web 12/14/2005

evidence for $Fe^{IV}_{aq}O^{2+}$ was more convincing, but still indirect.[12,14] Our own efforts allowed us to generate $Fe^{IV}_{aq}O^{2+}$ under similar conditions and characterize it by Mössbauer and XAS spectroscopy.[15] In a separate study, we examined the reactivity of $Fe^{IV}_{aq}O^{2+}$ toward a variety of organic substrates and found the oxidation of C−H bonds to occur in parallel hydrogen atom and hydride transfer steps.[16] In this work, we further explore the chemistry of $Fe^{IV}_{aq}O^{2+}$, particularly its reactivity in oxygen atom transfer reactions, which provides additional evidence for our formulation of this species as a pentaaquairon(IV)−oxo complex, $Fe(H_2O)_5O^{2+}$.

Experimental Section

Materials. The following chemicals were obtained from commercial sources at the highest purity available and were used as received: iron(II) tetrafluoroborate, iron(III) perchlorate, 1,10-phenanthroline, deuterated perchloric acid, methyl *p*-tolyl sulfoxide (TMSO), di(*p*-chlorophenyl) sulfoxide, methyl phenyl sulfoxide, titanium(IV) oxysulfate, deuterium oxide (from Aldrich); perchloric acid, dimethyl sulfoxide (DMSO), sodium acetate, acetonitrile, ammonium thiocyanate, hydrogen peroxide (from Fisher); ^{18}O water (98% enriched), dimethyl sulfoxide-d_6 (from CIL); sodium diphenylphosphinobenzene-3-sulfonate (TPPMS) (from TCI); and benzyl methyl sulfoxide (from Lancaster). Methyl *p*-chlorophenyl sulfoxide and methyl *p*-trifluoromethylphenyl sulfoxide were a generous gift from Prof. William S. Jenks at Iowa State University.

(2-Mercaptoethylamine-*N*,*S*)bis(ethylenediamine)cobalt(III) perchlorate ($CoSR^{2+}$) was available from a previous study.[17] Stock solutions of iron(II) perchlorate and ozone were prepared and standardized as previously described.[16] Ozone solutions contained ca. 0.5 mM O_3 and no detectable amounts of H_2O_2 (<2 μM) by titanium oxysulfate test.[16] Stock solutions of iron(II) were kept under argon, although under the conditions of this work (absence of coordinating anions) acidic solutions of Fe_{aq}^{2+} are air stable for at least several days. In-house distilled water was further purified with a Millipore Milli-Q system. The structural formulas of TPPMS and $CoSR^{2+}$ are shown below.

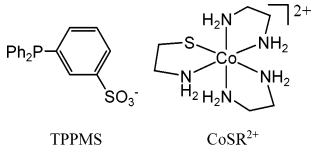

TPPMS $CoSR^{2+}$

Kinetics and Products. UV−vis kinetic studies were carried out with a Shimadzu UV-3101 PC spectrophotometer and Olis RSM-1000 stopped-flow apparatus at 25.0 ± 0.1 °C. All experiments were done in 0.10 M aqueous $HClO_4$, unless stated otherwise.

"Manual mixing" experiments consisted of initial premixing of Fe_{aq}^{2+} and O_3 in a magnetically stirred vial. The substrate was added quickly (within 0.2−0.5 s) from a preloaded syringe already in place and ready to be discharged. Fe_{aq}^{2+} yields were determined spectrophotometrically at 510 nm by the phenanthroline test, as previously described.[16] Occasionally, a correction was required for the absorption by iron(III)−phenanthroline complexes, in which case eq 3 was used (see Supporting Information for derivations of this and other equations).

Scheme 1

$$Fe_{aq}^{2+} + O_3 \rightarrow Fe^{IV}_{aq}O^{2+} + O_2 \qquad k = 8.3 \times 10^5\ M^{-1}\ s^{-1}$$

$$Fe^{IV}_{aq}O^{2+} \xrightarrow{Fe_{aq}^{2+}} 2\ Fe(III) \qquad k_{Fe} = 4.33 \times 10^4\ M^{-1}s^{-1}$$

$$Fe^{IV}_{aq}O^{2+} \xrightarrow{S^1} Fe_{aq}^{2+} + S^1O \qquad k_{S1}$$

Scheme 2

$$Fe_{aq}^{2+} + O_3 \xrightarrow{-O_2} Fe^{IV}_{aq}O^{2+} \xrightarrow{S^1} Fe_{aq}^{2+} + S^1O \qquad k_{S1}$$

$$Fe^{IV}_{aq}O^{2+} \xrightarrow{S^2} Fe_{aq}^{2+} + S^2O \qquad k_{S2}$$

$$[Fe(phen)_3^{2+}] = \frac{Abs_{510} \times R - Abs_{421}}{\epsilon_{510} \times R - \epsilon_{421}} \tag{3}$$

Here, ϵ_{510} and ϵ_{421} are molar absorptivities of $Fe(phen)_3^{2+}$ at 510 nm ($1.14 \times 10^4\ M^{-1}\ cm^{-1}$) and 421 nm ($6.4 \times 10^3\ M^{-1}\ cm^{-1}$), and $R = 7.46$ is the ratio of molar absorptivities at 421 and 510 nm for phenanthroline complexes of iron(III). Mixtures of authentic samples of Fe_{aq}^{3+} and Fe_{aq}^{2+} at known concentrations showed less than 0.5% error in the Fe_{aq}^{2+} concentration determined by this method. In the absence of UV-absorbing substrates, the concentration of Fe_{aq}^{3+} was determined spectrophotometrically at 240 nm, $\epsilon_{240} = 4160\ M^{-1}\ cm^{-1}$. Otherwise, concentrations of Fe_{aq}^{3+} in the range 0−200 μM were determined by adding 0.2 M NH_4SCN to the sample, measuring the absorbance at 480 and 700 nm, and calculating the concentration of iron(III)-thiocyanate from the difference, $(\epsilon_{480} - \epsilon_{700}) = 8.52 \times 10^3\ M^{-1}\ cm^{-1}$.

For competition studies, ozone was introduced into a mixture of organic substrates and Fe_{aq}^{2+}. The products, i.e., Fe_{aq}^{2+}, Fe_{aq}^{3+}, and oxidized organic materials, were quantified by the methods described below. A large excess of competing substrates with respect to the initial O_3 concentration was used to maintain pseudo-first-order conditions in most cases.

In one scenario, Fe_{aq}^{2+} ($k_{Fe} = 4.33 \times 10^4\ M^{-1}\ s^{-1}$)[16] and the substrate of interest (k_{S1}) were allowed to compete for $Fe^{IV}_{aq}O^{2+}$, Scheme 1. The rate constant k_{S1} was calculated from the yields of Fe_{aq}^{3+} by fitting the data to eq 4, where k_{Fe} represents the overall rate constant for the disappearance of $Fe_{aq}O^{2+}$. The rate constants for the two individual pathways in the reaction between Fe_{aq}^{2+} and $Fe^{IV}_{aq}O^{2+}$ are $3.56 \times 10^4\ M^{-1}\ s^{-1}$ (formation of Fe_{aq}^{3+}) and $7.7 \times 10^3\ M^{-1}\ s^{-1}$ (formation of $Fe_{aq}(OH)_2Fe_{aq}^{4+}$).[16]

$$\frac{1}{[Fe^{3+}]_\infty} = \frac{1}{2[O_3]_0}\left[1 + \frac{k_{S1}[S1]_0}{k_{Fe}[Fe^{2+}]_0}\right] \tag{4}$$

Alternatively, two substrates, S1 and S2, were allowed to compete for $Fe^{IV}_{aq}O^{2+}$, while the concentration of Fe_{aq}^{2+} was kept low to prevent the $Fe^{IV}_{aq}O^{2+}/Fe_{aq}^{2+}$ reaction, Scheme 2 and eq 5.

$$[S2]_\infty = [O_3]_0 \frac{k_{S2}[S2]_0}{k_{S2}[S2]_0 + k_{S1}[S1]_0} \tag{5}$$

(14) Loegager, T.; Holcman, J.; Sehested, K.; Pedersen, T. *Inorg. Chem.* **1992**, *31*, 3523−3529.
(15) Pestovsky, O.; Stoian, S.; Bominaar, E. L.; Shan, X.; Münck, E.; Que, L., Jr.; Bakac, A. *Angew. Chem., Int. Ed.* **2005**, *44*, 6871−6874.
(16) Pestovsky, O.; Bakac, A. *J. Am. Chem. Soc.* **2004**, *126*, 13757−13764.
(17) Huston, P.; Espenson, J. H.; Bakac, A. *Inorg. Chem.* **1993**, *32*, 4517−4523.

The competing substrate S2 was usually DMSO, for which the rate constant k_{S2} was determined first by the approach outlined in Scheme 1. GC−MS experiments with DMSO in $H_2{}^{18}O$ were carried out as follows: 0.5 mL of a solution containing DMSO, $Fe_{aq}{}^{2+}$, and $HClO_4$ in $H_2{}^{18}O$ was placed in a 3-mL vial. Ozone was bubbled continuously for a set time, chosen to allow 10−30% of DMSO to be oxidized, as determined in parallel experiments with methyl *p*-tolyl sulfoxide under identical conditions. The methyl *p*-tolyl sulfone generated in this reaction absorbs strongly in the UV, which allowed us to determine its yields precisely in direct spectrophotometric measurements. The yields so determined are directly applicable to DMSO, because the two sulfoxides have almost identical rate constants for the reaction with $Fe^{IV}{}_{aq}O^{2+}$, see later.

Large yields of methyl sulfone were necessary to obtain a good signal-to-noise ratio in GC−MS spectra, but the degree of oxidation was kept below 30% to maintain nearly pseudo-first-order conditions. Ozone bubbling times varied between 10 s (7.0 mM $Fe_{aq}{}^{2+}$) and 1 min (0.40 mM $Fe_{aq}{}^{2+}$) and depended on the initial concentration of $Fe_{aq}{}^{2+}$ but not that of DMSO. When ozone bubbling was finished, the solution was neutralized with concentrated Na_2CO_3, and GC−MS spectra were recorded on Finnigan TSQ700 and Varian Saturn 2000 instruments in EI mode (see Supporting Information for typical GC−MS spectra). The spectrum of the sole organic product, methyl sulfone, had the largest peak at $m/z = 94$ (molecular ion) for the TSQ700 instrument (triple quad MS), or $m/z = 95$ for the Saturn 2000 instrument (ion trap MS). The larger mass in the latter is caused by the protonation of the molecular ion by water in the ion trap chamber and was confirmed with authentic samples of methyl sulfone. Corresponding peaks for the labeled product $(CH_3)_2S(^{16}O)(^{18}O)$ appeared at $m/z = 96$ and 97 for the TSQ700 and Saturn 2000 instruments, respectively. After correction for a small amount of $H_2{}^{16}O$ in the samples, the ratio of peak intensities at $m/z = 94$ and 96 (or $m/z = 95$ and 97) was used to calculate the yield of the labeled product. The results obtained with two different GC−MS instruments agreed to within 10% of each other.

The reaction between TPPMS and $Fe^{IV}{}_{aq}O^{2+}$ was carried out in a home-built stopped-flow setup consisting of two teflon inlet tubes, attached to a mixing chamber, and two outlet teflon tubes. The reagents, $Fe_{aq}{}^{2+}$ (0.19 mM) and O_3 (0.17 mM), were introduced by simultaneous manual injection through inlet tubes. A small excess of $Fe_{aq}{}^{2+}$ over O_3 ensured that the resulting mixtures contained no residual ozone, which would oxidize TPPMS directly. The output from one outlet tube was injected into a stirred solution of 50−100 mM DMSO. The concentration of $Fe_{aq}{}^{2+}$ generated in this reaction was used to calculate the initial concentration of $Fe^{IV}{}_{aq}O^{2+}$, which was reproducibly 0.14−0.15 mM. The output from the second outlet tube was injected into a stirred TPPMS/DMSO mixture. Control runs, in which both outlet streams were mixed with high concentrations of DMSO, agreed to within 5% of each other. The resulting product mixtures were immediately purged with argon and placed in NMR tubes.

^1H and ^{31}P NMR spectra were recorded with a Varian VXR400 instrument at room temperature against external TMS and H_3PO_4 as standards, respectively. A solvent mixture of 30% D_2O and 70% H_2O was used to obtain deuterium lock in ^{31}P NMR experiments. For TPPMS experiments, samples were purged with argon, capped with rubber septa, and sealed with Parafilm to prevent autoxidation. Collection times of up to 6 h were used. Control experiments showed no significant phosphine oxidation by air under these conditions.

NMR experiments with $CoSR^{2+}$ were carried out in D_2O, which was acidified with concentrated $DClO_4$. Authentic samples of $CoS(O)R^{2+}$ and $CoS(O)_2R^{2+}$ suitable for NMR analysis were prepared by controlled oxidation of $CoSR^{2+}$ by hydrogen peroxide.[18] The concentration of $CoS(O)R^{2+}$ was determined by UV−vis spectrophotometry at 365 nm, $\epsilon_{365} = 6500\ M^{-1}\ cm^{-1}$.

Kinetic simulations were done with Chemical Kinetics Simulator 1.01 software. Rate constants determined in this study, as well as those from our previous work,[16] were used in conjunction with the reaction mechanism shown in Scheme 3 to calculate the yields of $Fe^{IV}{}_{aq}O^{2+}$ and oxidized substrates. Nonlinear least-squares fittings were done with Kaleidagraph 3.51 software.

Scheme 3

$Fe_{aq}{}^{2+} + O_3 \rightarrow Fe^{IV}{}_{aq}O^{2+} + O_2$	$8.3 \times 10^5\ M^{-1}\ s^{-1}$
$Fe^{IV}{}_{aq}O^{2+} + S \rightarrow Fe_{aq}{}^{2+} + SO$	k_S
$Fe^{IV}{}_{aq}O^{2+} + S\ (+ 2H^+) \rightarrow Fe_{aq}{}^{3+} + "S^{+n}" + H_2O$	k_P
$Fe^{IV}{}_{aq}O^{2+} + Fe_{aq}{}^{2+}\ (+ 2H^+) \rightarrow 2Fe_{aq}{}^{3+} + H_2O$	$3.56 \times 10^4\ M^{-1}\ s^{-1}$
$Fe^{IV}{}_{aq}O^{2+} + Fe_{aq}{}^{2+}\ (+ H_2O) \rightarrow Fe_{aq}(OH)_2Fe_{aq}{}^{4+}$	$7.7 \times 10^3\ M^{-1}\ s^{-1}$
$Fe^{IV}{}_{aq}O^{2+} + H^+ \rightarrow Fe_{aq}{}^{3+} + 1/4\ O_2 + 1/2\ H_2O$	$0.10\ s^{-1}$

Table 1. Kinetics Data ($M^{-1}\ s^{-1}$) for Oxidations by Ozone and $Fe^{IV}{}_{aq}O^{2+}$ in 0.10 M Aqueous $HClO_4$

substrate	k_{O3}[a]	$k_{Fe(IV)}/10^5$ [a]
DMSO	22	1.26
DMSO-d_6	*b*	1.23
p-CH_3-C_6H_4-S(O)-CH_3	14	1.16
C_6H_5-S(O)-CH_3	*b*	1.23
p-Cl-C_6H_4-S(O)-CH_3	*b*	0.99
p-CF_3-C_6H_4-S(O)-CH_3	*b*	0.79
C_6H_5-CH_2-S(O)-CH_3	*b*	1.48
$(p\text{-Cl-}C_6H_4)_2SO$	*b*	∼0.7
TPPMS	$>2 \times 10^7$	∼200
$CoSR^{2+}$	$>6 \times 10^7$	∼100
$CoS(O)R^{2+}$	5.60×10^6	∼1300

[a] Uncertainties: 5−7%. [b] Not determined.

Results

Reactions with Ozone. The kinetics of the oxidation of DMSO (1.17−2.33 mM) were monitored at the 260-nm maximum of O_3 under pseudo-first-order conditions. Kinetic traces were nearly exponential, although some tailing near the end of the reaction was observed. For fitting purposes, the traces were cut at six half-lives and fitted to an exponential rate equation. The second-order rate constant for the reaction between O_3 and DMSO, obtained from the slope of a plot of pseudo-first-order rate constants against DMSO concentration, is $k_6 = 22 \pm 1\ M^{-1}\ s^{-1}$, eq 6 (R = CH_3). A similar set of experiments yielded $k_6 = 14 \pm 1\ M^{-1}\ s^{-1}$ for methyl *p*-tolyl sulfoxide (R = 4-CH_3−C_6H_4), Table 1.

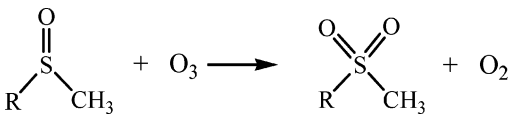

(6)

The reaction between TPPMS (23 μM) and O_3 (5 μM) was complete in the stopped-flow mixing time, placing the lower limit for the rate constant k_7 at $>2 \times 10^7\ M^{-1}\ s^{-1}$, eq 7.

(18) Adzamli, I. K.; Libson, K.; Lydon, J. D.; Elder, R. C.; Deutsch, E. *Inorg. Chem.* **1979**, *18*, 303−311.

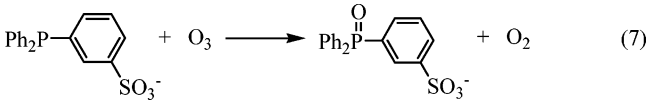

(7)

The reaction between $CoSR^{2+}$ (1.0−2.6 μM) and O_3 (6.6−12.6 μM) was also complete in the stopped-flow mixing time, as was indicated by the instantaneous rise of absorbance at 365 nm caused by the formation of $CoS(O)R^{2+}$. Subsequent exponential absorbance decrease (50−100 ms) was attributed to the further oxidation of $CoS(O)R^{2+}$. These data yielded the rate constants for the two consecutive processes, $k_8 > 6 \times 10^7$ M^{-1} s^{-1} and $k_9 = (5.60 \pm 0.06) \times 10^6$ M^{-1} s^{-1}.

$$CoSR^{2+} + O_3 \rightarrow CoS(O)R^{2+} + O_2 \quad (8)$$

$$CoS(O)R^{2+} + O_3 \rightarrow CoS(O)_2R^{2+} + O_2 \quad (9)$$

Reactions with $Fe^{IV}_{aq}O^{2+}$. In the experiments utilizing "manual mixing" (see Experimental Section), 127 μM Fe_{aq}^{2+} and 100 μM O_3 were premixed to generate (theoretically) 73 μM $Fe^{IV}_{aq}O^{2+}$ (i.e., the reaction initially generates 100 μM $Fe^{IV}_{aq}O^{2+}$, of which 27 μM is rapidly consumed by excess Fe_{aq}^{2+}). After adding 0.47 M DMSO, 52 μM Fe_{aq}^{2+} was regenerated. This represents a 70% yield in a reaction taking place, as in eq 10. Similar reactions with 1.8 mM $CoSR^{2+}$ and with 1.9 mM TPPMS yielded 61 μM (84%) and 69 μM (94%) of Fe_{aq}^{2+}. Yields of Fe_{aq}^{2+} below 100% are easily explained by less-than-perfect mixing in this type of experiments and by the short lifetime of $Fe^{IV}_{aq}O^{2+}$ ($t_{1/2}$ = 7 s). As shown later, yields were much closer to theoretical in all of the experiments utilizing the more efficient stopped-flow mixing. The oxidation of $CoSR^{2+}$ yielded 35 μM $CoS(O)R^{2+}$, the rest being overoxidized to $CoS(O)_2R^{2+}$.

$$Fe_{aq}^{2+} + O_3 \xrightarrow{-O_2} Fe_{aq}O^{2+} \xrightarrow{S} Fe_{aq}^{2+} + SO \quad (10)$$

A clear demonstration of quantitative oxygen atom transfer from $Fe^{IV}_{aq}O^{2+}$ to sulfoxides is provided by our ability to run the reaction in the catalytic mode, Scheme 4, as shown in Figure 1.

In the absence of Fe_{aq}^{2+}, the oxidation of 100 μM methyl *p*-tolyl sulfoxide (TMSO) with 100 μM O_3 required more than 5000 s and yielded 90% sulfone. In the presence of 2 and 5 μM Fe_{aq}^{2+}, the reaction was complete in several seconds and gave 87 and 100%, respectively, of methyl *p*-tolyl sulfone. The much shorter times required for the completion of the reaction in the presence of Fe_{aq}^{2+} clearly rule out a direct O_3/sulfoxide reaction under those conditions, and the small required amount of Fe_{aq}^{2+} for quantitative oxidation requires a turnover number of at least 20. The

Scheme 4

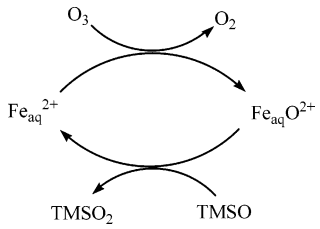

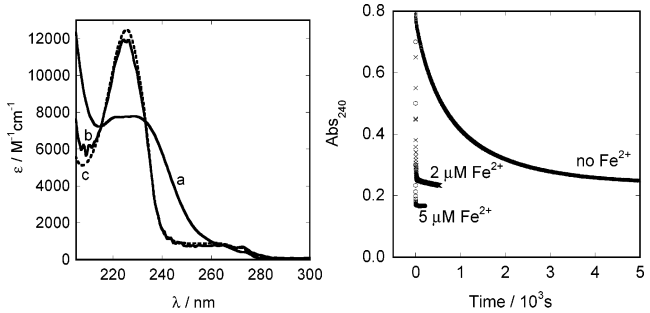

Figure 1. Oxidation of 100 μM methyl *p*-tolyl sulfoxide with 100 μM ozone catalyzed by Fe_{aq}^{2+} in 0.10 M aqueous $HClO_4$. Spectra: (a) methyl *p*-tolyl sulfoxide, (b) methyl *p*-tolyl sulfone obtained by oxidation of **a** by O_3, and (c) methyl *p*-tolyl sulfone obtained by Fe_{aq}^{2+}-catalyzed oxidation of **a** by O_3. Kinetic traces at 240 nm at 0 μM Fe_{aq}^{2+}, 2 μM Fe_{aq}^{2+}, and 5 μM Fe_{aq}^{2+}.

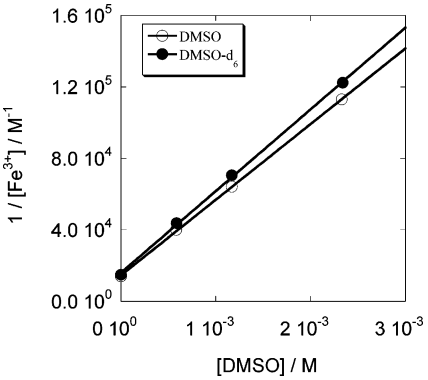

Figure 2. Reciprocals of the yields of Fe_{aq}^{3+} produced in the reaction between 1.0 mM Fe_{aq}^{2+} and 35 μM O_3 in the presence of 0−2.4 mM DMSO in 0.10 M aqueous $HClO_4$. Experimental data were fitted to eq 4.

elementary step of eq 10 thus has to be ≫99% efficient; the loss of even 1% of $Fe^{IV}_{aq}O^{2+}$ or Fe_{aq}^{2+} per cycle (as in step k_P in Scheme 3) would cut the yield of sulfone to 80% in the experiment with $[Fe_{aq}^{2+}]_0 = 5$ μM.

Kinetics of Sulfoxide Oxidations by Competition Methods. An attempt was made to study the kinetics of substrate/$Fe^{IV}_{aq}O^{2+}$ reactions by stopped-flow mixing, but even at the lowest substrate concentrations used, all of the reactions were complete in the stopped-flow mixing time. Thus, we resorted to competition methods to obtain kinetics data.

Upon the addition of ozone to a mixture of Fe_{aq}^{2+} and a sulfoxide, $Fe^{IV}_{aq}O^{2+}$ is generated "instantaneously." The subsequent competition between Fe_{aq}^{2+} and sulfoxides for $Fe^{IV}_{aq}O^{2+}$, Scheme 1, is demonstrated for DMSO in Figure 2. As expected for this reaction scheme, the yields of Fe_{aq}^{3+} decreased as the concentration of DMSO was raised and were below the detection limit at >50 mM DMSO (complete Fe_{aq}^{2+} recovery). A fit of the experimental data to eq 4 afforded the second-order rate constant for the oxidation of DMSO by $Fe^{IV}_{aq}O^{2+}$, $k_{11} = (1.26 \pm 0.06) \times 10^5$ M^{-1} s^{-1}. Within the experimental error, there is no deuterium isotope effect. The rate constant for DMSO-d_6 is $k_{12} = (1.23 \pm 0.09) \times 10^5$ M^{-1} s^{-1}, eqs 11 and 12.

$$(CH_3)_2SO + Fe^{IV}_{aq}O^{2+} \rightarrow (CH_3)_2SO_2 + Fe_{aq}^{2+} \quad (11)$$

$$(CD_3)_2SO + Fe^{IV}_{aq}O^{2+} \rightarrow (CD_3)_2SO_2 + Fe_{aq}^{2+} \quad (12)$$

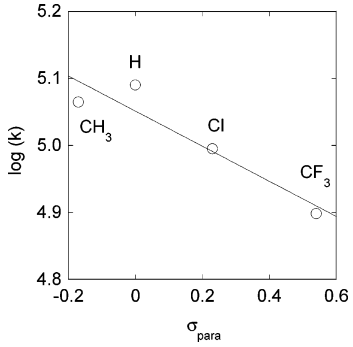

Figure 3. Hammett correlation for the reaction between $Fe^{IV}_{aq}O^{2+}$ and para-substituted methyl phenyl sulfoxides in 0.10 M aqueous $HClO_4$.

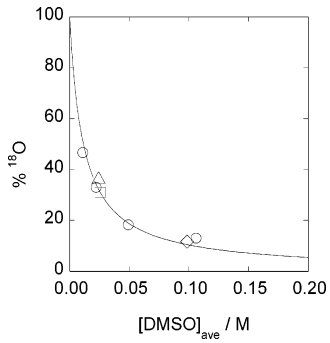

Figure 4. Yields of $(CH_3)_2S(^{16}O)(^{18}O)$ obtained by oxidation of DMSO with $Fe^{IV}_{aq}O^{2+}$ in acidic $H_2{}^{18}O$ under continuous bubbling with $^{16}O_3$. $[HClO_4] = 0.10$ M (○), 0.21 M (△), and 0.054 M (□). $[Fe_{aq}{}^{2+}] = 7.0$ mM (◊) or 0.40 mM (○, △, □). Fit to eq 13 is shown.

A similar procedure was used for the reactions of $Fe^{IV}_{aq}O^{2+}$ with aromatic sulfoxides, except that the yields of $Fe_{aq}{}^{3+}$ were determined by the thiocyanate method. Direct determination of $Fe_{aq}{}^{3+}$ from the absorbance at 240 nm was ruled out by intense UV absorption by aromatic substrates. Only an estimate of the rate constant for the reaction with di(*p*-chlorophenyl) sulfoxide was obtained because of the low solubility of this substrate in water. Kinetic data for all of the sulfoxides studied are summarized in Table 1. A Hammett correlation for para-substituted methyl phenyl sulfoxides is shown in Figure 3, which afforded a Hammett reaction constant $\rho = -0.26 \pm 0.07$.

Oxygen Exchange Between $Fe^{IV}_{aq}O^{2+}$ and Water. Oxidation of DMSO by O_3 in $H_2{}^{18}O$ was carried out in the presence of catalytic amounts of $Fe_{aq}{}^{2+}$, 0.40−7.0 mM. At low DMSO concentrations, a significant amount of ^{18}O incorporation into methyl sulfone was observed by GC−MS (see Supporting Information). As the concentration of DMSO was increased, the proportion of the labeled sulfone decreased, as shown in Figure 4. The experimental data were fitted to the expression for competition kinetics in eq 13 and gave $k_{ex} = (1.4 \pm 0.1) \times 10^3\ s^{-1}$.

$$\%^{18}O = 100\frac{k_{ex}}{k_{ex} + k_{DMSO}[DMSO]} \qquad (13)$$

Oxidation of TPPMS and $CoSR^{2+}$. Unlike sulfoxides, both of these substrates react rapidly with O_3, which ruled out the use of catalytic conditions to accumulate large amounts of products for spectroscopic measurements. Instead, these experiments used 1 mM TPPMS and 0.14−0.15 mM $Fe^{IV}_{aq}O^{2+}$ (generated in situ) and stopped-flow mixing. After the completion of the reaction, the ^{31}P NMR spectrum exhibited a new resonance at 37.8 ppm, corresponding to TPPMS oxide. The only other resonance observed was that at −3.9 ppm, corresponding to excess TPPMS, see Supporting Information. The reaction can thus be written as in eq 14.

Table 2. Product of Oxidation of $CoSR^{2+}$ by $Fe^{IV}_{aq}O^{2+}$ in the Presence and Absence of DMSO in 0.10 M $HClO_4$

	reactants/mM			products/mM		
series	$Fe^{IV}_{aq}O^{2+}$ [a]	$CoSR^{2+}$	DMSO	$Fe_{aq}{}^{2+}$ [b]	$CoS(O)R^{2+}$ [c]	$CoS(O)_2R^{2+}$ [d]
1[e]	0.28	0.51	0	0.28	traces	0.14
2	0.055	0.65	0	0.051	0.031	*f*
3	0.21	2.1	0	0.21	0.100	*f*
	0.21	2.1	540	0.22	0.044	*f*
	0.21	2.1	900	0.21	0.021	*f*
	0.21	2.1	1350	0.21	0.020	*f*

[a] Generated by stopped-flow mixing of $Fe_{aq}{}^{2+}$ and ozone. [b] Phenanthroline test. [c] UV−vis at 365 nm. [d] NMR. [e] In $D_2O/DClO_4$. [f] Not determined.

$$TPPMS + Fe^{IV}_{aq}O^{2+} \rightarrow TPPMSO + Fe_{aq}{}^{2+} \qquad (14)$$

The concentration of TPPMS oxide, obtained from the peak intensity, was 93% of the initial concentration of $Fe^{IV}_{aq}O^{2+}$. This yield decreased to only 51% when the oxidation was carried out in the presence of 0.10 M DMSO, consistent with the competition shown in Scheme 2. Since the amount of generated TPPMS oxide is limited by the initial concentration of $Fe^{IV}_{aq}O^{2+}$, which in turn is limited by the solubility of ozone in water, the signal-to-noise ratio of the NMR data was low and was only suitable to obtain an estimate for the rate constant, $k_{14} \approx 2 \times 10^7\ M^{-1}\ s^{-1}$.

The products of oxidation of $CoSR^{2+}$ by $Fe^{IV}_{aq}O^{2+}$ were analyzed by UV−vis and ^1H NMR spectroscopies, see Supporting Information. To improve the signal-to-noise ratio in NMR experiments, we used the maximum obtainable concentrations of $Fe^{IV}_{aq}O^{2+}$ and comparable amounts of $CoSR^{2+}$. Such conditions favored further oxidation of $CoS(O)R^{2+}$ to $CoS(O)_2R^{2+}$, eqs 15 and 16. As a result, the yields of $CoS(O)R^{2+}$ were quite small (Series 1, Table 2). As mentioned earlier, the yields of $Fe_{aq}{}^{2+}$ were ∼100% in all of the experiments in Table 2.

$$CoSR^{2+} + Fe^{IV}_{aq}O^{2+} \rightarrow CoS(O)R^{2+} + Fe_{aq}{}^{2+} \qquad (15)$$

$$CoS(O)R^{2+} + Fe^{IV}_{aq}O^{2+} \rightarrow CoS(O)_2R^{2+} + Fe_{aq}{}^{2+} \qquad (16)$$

For spectrophotometric determinations, much lower $[Fe^{IV}_{aq}O^{2+}]$ and higher $[CoSR^{2+}]$ could be used. These conditions produced larger relative yields of $CoS(O)R^{2+}$ (56% in Series 2, Table 2).

Series 3 in Table 2 represents a set of experiments where a competition for $Fe^{IV}_{aq}O^{2+}$ was set up between $CoSR^{2+}$ and DMSO. The data were fitted to the expression for competition kinetics in eq 17, which disregards further oxidation of $CoS(O)R^{2+}$. The fit gave $k_{15} = (2.0 \pm 0.5) \times 10^7\ M^{-1}\ s^{-1}$.

$$\frac{1}{[CoS(O)R^{2+}]} = \frac{1}{[Fe_{aq}O^{2+}]_0}\left(1 + \frac{k_{DMSO}[DMSO]}{k_{15}[CoSR^{2+}]_{avg}}\right) \quad (17)$$

Kinetics simulations were used to further refine the values of rate constants in reactions 15 and 16. A good agreement between experimental and simulated data was found by adjusting k_{15} and k_{16} until the calculated yields of $CoS(O)R^{2+}$ and $CoS(O)_2R^{2+}$ matched the experimental yields. This treatment gave $k_{15} \approx 1 \times 10^7$ M^{-1} s^{-1} and $k_{16} \approx 1.3 \times 10^8$ M^{-1} s^{-1} (see Supporting Information).

Discussion

The evidence for oxygen atom transfer from $Fe^{IV}_{aq}O^{2+}$ to various substrates comes from several different series of experiments. In all of the cases studied—sulfoxides, $CoSR^{2+}$, and phosphine—the oxidation by $Fe^{IV}_{aq}O^{2+}$ generated stoichiometric amounts of Fe_{aq}^{2+}. Even though Fe_{aq}^{2+} is both the source of $Fe^{IV}_{aq}O^{2+}$ in these experiments and the final product, the separation of various processes and kinetic steps is straightforward, as explained for each individual case in the Experimental Section, Results, and Supporting Information.

As already pointed out, the catalytic cycle shown in Figure 1 and Scheme 4 is a particularly convincing argument for oxygen atom transfer. At the least, the experiment provides undeniable evidence for the cycling between Fe_{aq}^{2+} and $Fe^{IV}_{aq}O^{2+}$ in the process of oxidation of TMSO to $TMSO_2$ by O_3. Although unlikely, the $Fe_{aq}^{2+}/Fe^{IV}_{aq}O^{2+}$ cycling could take place by a mechanism other than oxygen atom transfer. One could consider hydride transfer, for example, but this mechanism is all but ruled out by the lack of the deuterium isotope effect, $k_H/k_D = 1.02 \pm 0.09$, Table 1. Also, we are not aware of any precedents for hydride transfer from sulfoxides. By far the strongest argument for oxygen atom transfer comes from the ^{18}O-labeling experiments and oxo oxygen exchange, as described below.

Oxygen Exchange. Kinetic determinations in the presence and absence of Fe_{aq}^{2+} (Table 1 and Figure 1) and kinetic simulations have established that the direct DMSO/O_3 reaction, under the conditions used in oxygen exchange experiments, could not account for more than 1% of the total product and that the $Fe^{IV}_{aq}O^{2+}$/DMSO reaction was the source of >99% of methyl sulfone. In addition, the observed pattern of ^{18}O incorporation, and the effect of $[Fe_{aq}^{2+}]$ and [DMSO] on this pattern, definitely rule out measurable contribution from the direct reaction.

The total amount of the sulfone produced in a given amount of time was independent of [DMSO] but increased with the initial concentration of Fe_{aq}^{2+} (catalyst). At the same time, the ratio of labeled to unlabeled methyl sulfone was independent of the initial concentrations of Fe_{aq}^{2+} and acid but varied with [DMSO], as shown in Figure 4. All of these results are exactly as predicted by the mechanism in Scheme 5.

An initial fast reaction[16] between isotopically labeled $Fe(H_2{}^{18}O)_6^{2+}$ and $^{16}O_3$ in $H_2{}^{18}O$ gives $(H_2{}^{18}O)_5Fe^{16}O^{2+}$. This species can either transfer ^{16}O directly to DMSO and give

Scheme 5

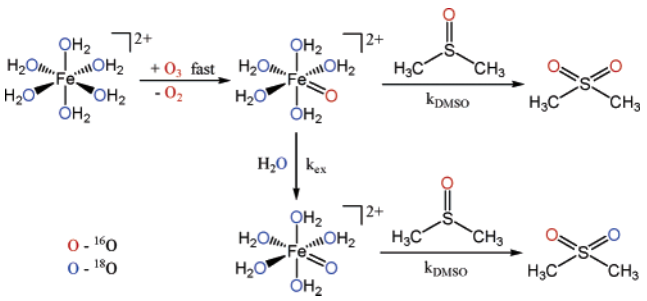

DMSO(^{16}O), or exchange the oxo oxygen with $H_2{}^{18}O$ to give $(H_2{}^{18}O)_5Fe(^{18}O)^{2+}$, which will transfer ^{18}O to DMSO and yield DMSO(^{18}O). The larger the concentration of DMSO, the faster the $Fe^{IV}_{aq}O^{2+}$/DMSO reaction and the smaller the chance for oxygen exchange with solvent water. In the (extrapolated) limit of very high [DMSO], there would be no oxygen exchange with $H_2{}^{18}O$, and all of the sulfone should be DMSO(^{16}O). The highest experimental yield of DMSO(^{16}O) was 88%, obtained at 0.12 M DMSO. Inconveniently high concentrations of DMSO would be required for a greater percentage of ^{16}O incorporation in competition with the very rapid $Fe^{IV}_{aq}O^{2+}/H_2O$ oxo group exchange, $k = 1.4 \times 10^3$ s^{-1}.

The observed 88% yield of DMSO(^{16}O) allows us to dismiss the formulation of aquaferryl(IV) ion as other than $Fe^{IV}_{aq}O^{2+}$. One might consider, for example, a dihydroxy species, $Fe_{aq}(OH)_2^{2+}$, in which, by experimental design, at least one of the two hydroxo groups would have to be derived from $H_2{}^{18}O$. Having two chemically equivalent but isotopically different hydroxyl groups in the molecule would require the yield of DMSO(^{16}O) to be no more than 50%. The nearly quantitative experimental yield is consistent only with a species which contains one unique oxygen. This feature, combined with the Mössbauer spectrum,[15] an overall 2+ charge,[16] and DFT calculations[15] strongly support the $Fe^{IV}_{aq}O^{2+}$ formulation.

The reaction with aromatic sulfoxides exhibits a negative Hammett (ρ) value, indicative of a build-up of a positive charge at sulfur in the transition state, consistent with electrophilic attack by $Fe^{IV}_{aq}O^{2+}$. The high reactivity of $Fe^{IV}_{aq}O^{2+}$ in such reactions is responsible for the small absolute value of ρ, i.e., for the low selectivity of $Fe^{IV}_{aq}O^{2+}$.

The rate constant for the reaction with $CoS(O)R^{2+}$ ($k = 1.3 \times 10^8$ M^{-1} s^{-1}) is one of the largest reported for oxygen atom transfer from a metal–oxo species. Some other examples of fast oxygen atom transfer include the reactions between oxorhenium(VII)–dioxazoline complex and triphenylphosphine ($k > 10^6$ M^{-1} s^{-1}),[19] oxoiron(IV)–porphyrin radical cation complex and *p*-methoxythioanisole ($k = 1.7 \times 10^4$ M^{-1} s^{-1} at −50 °C),[20] and oxomanganese(V)–porphyrin complex and bromide (estimated $k = 10^8$ M^{-1} s^{-1}).[21]

Although there are a number of reports on oxygen exchange between a metal–oxo group and water, quantitative

(19) McPherson, L. D.; Drees, M.; Khan, S. I.; Strassner, T.; Abu-Omar, M. M. *Inorg. Chem.* **2004**, *43*, 4036–4050.
(20) Goto, Y.; Matsui, T.; Ozaki, S.-i.; Watanabe, Y.; Fukuzumi, S. *J. Am. Chem. Soc.* **1999**, *121*, 9497–9502.

kinetics data for such reactions are rare.[22−29] From the few rate constants that have been measured, it is obvious that these values are a function of the metal, its oxidation state, and the ligand environment, which makes a direct comparison to $Fe^{IV}_{aq}O^{2+}$ rather difficult to make. The closest example in the literature is the exchange between traces of water in acetonitrile and the iron(IV)−oxo complex of tetramethylcyclam, for which the rate constant of $5.4 \pm 0.6\ M^{-1}\ s^{-1}$ was reported.[29] Oxygen exchange was proposed to occur directly between the oxo group and the water molecule, without the involvement of other ligands.

If the k_{ex} obtained in this study is divided by the concentration of solvent water, one obtains an estimate for the second-order rate constant for bimolecular oxygen exchange between $Fe^{IV}_{aq}O^{2+}$ and water, $k_{exch} = 25 \pm 2\ M^{-1}\ s^{-1}$. This value is less than an order of magnitude smaller than that for the tetramethylcyclam complex and may suggest a similar mechanism of oxygen exchange. On the other hand, the similarity in rate constants may be purely coincidental, and $Fe^{IV}_{aq}O^{2+}$ may utilize the oxo−hydroxo tautomerism, a mechanism that appears to dominate oxygen exchange chemistry of oxo−porphyrin complexes of iron and manganese.[30] Applied to $Fe^{IV}_{aq}O^{2+}$, the mechanism could be written as:

$$(H_2{}^{18}O)_5Fe(^{16}O)^{2+} \rightleftharpoons (H_2{}^{18}O)_4Fe(^{16}OH)(^{18}OH)^{2+} \rightleftharpoons (H_2{}^{18}O)_4(H_2{}^{16}O)Fe(^{18}O)^{2+}$$

$$-H_2{}^{16}O \downarrow + H_2{}^{18}O\ (\text{solvent})$$

$$(H_2{}^{18}O)_5Fe(^{18}O)^{2+}$$

Even though our data clearly rule out the dihydroxy complex as a dominant or reactive form in oxygen atom transfer reactions, such a complex may be involved as a transient or the transition state for oxo exchange.

Acknowledgment. We are grateful to Prof. W. S. Jenks for a gift of substituted sulfoxides. This manuscript has been authored by Iowa State University under Contract No. W-7405-ENG-82 with the U.S. Department of Energy.

Supporting Information Available: Experimental detail, MS and NMR spectra, and kinetic derivations. This material is available free of charge via the Internet at http://pubs.acs.org.

IC051868Z

(21) Jin, N.; Bourassa, J. L.; Tizio, S. C.; Groves, J. T. *Angew. Chem., Int. Ed.* **2000**, *39*, 3849−3851.
(22) Astashkin, A. V.; Feng, C.; Raitsimring, A. M.; Enemark, J. H. *J. Am. Chem. Soc.* **2005**, *127*, 502−503.
(23) Comba, P.; Merbach, A. *Inorg. Chem.* **1987**, *26*, 1315−1323.
(24) Hinch, G. D.; Wycoff, D. E.; Murmann, R. K. *Polyhedron* **1986**, *5*, 487−495.
(25) Johnson, M. D.; Murmann, R. K. *Inorg. Chem.* **1983**, *22*, 1068−1072.
(26) Nam, W.; Valentine, J. S. *J. Am. Chem. Soc.* **1993**, *115*, 1772−1778.
(27) Rahmoeller, K. M.; Murmann, R. K. *Inorg. Chem.* **1983**, *22*, 1072−1077.
(28) Rodgers, K. R.; Murmann, R. K.; Schlemper, E. O.; Shelton, M. E. *Inorg. Chem.* **1985**, *24*, 1313−1322.
(29) Seo, M. S.; In, J.-H.; Kim, S. O.; Oh, N. Y.; Hong, J.; Kim, J.; Que, L., Jr.; Nam, W. *Angew. Chem., Int. Ed.* **2004**, *43*, 2417−2420.
(30) Meunier, B.; Bernadou, J. *Top. Catal.* **2002**, *21*, 47−54.